Influence of Structural Fluctuation on Enzyme Reaction Energy Barriers in Combined Quantum Mechanical/Molecular Mechanical Studies

Yingkai Zhang,* Jeremy Kua, and J. Andrew McCammon

Howard Hughes Medical Institute, Department of Chemistry and Biochemistry, and Department of Pharmacology, University of California at San Diego, La Jolla, California 92093-0365

Received: December 5, 2002; In Final Form: February 17, 2003

To account for protein dynamics and to investigate the effect of different conformations on the enzyme reaction energy barrier, we have studied the initial step of the acylation reaction catalyzed by acetylcholinesterase (AChE) with a multiple QM/MM reaction path approach. The approach consists of two main components: generating enzyme−substrate conformations with classical molecular dynamics simulation and mapping out the minimum reaction energy path for each conformational snapshot with combined quantum mechanical/molecular mechanical (QM/MM) calculations. It is found that enzyme−substrate conformation fluctuations lead to significant differences in the calculated reaction energy barrier; however, the qualitative picture of the role of the catalytic triad and oxyanion hole in AChE catalysis is very consistent. Our results emphasize the importance of employing multiple starting structures in the QM/MM study of enzyme reactions and indicate that structural fluctuation is an integral part of the enzyme reaction process.

1. Introduction

Enzymes are powerful and complex. They catalyze a wide variety of chemical reactions with remarkable efficiency and specificity.[1] Over the decades, intense experimental and theoretical efforts have been devoted to the understanding of the structural origin of enzyme activity. Simultaneously, our view of biological macromolecules has changed considerably. Many experimental and computational studies have provided convincing evidence that the structural dynamics of proteins are crucial for function.[2−7] Under native conditions, a protein in solution undergoes a variety of constant random thermal motions and conformational transitions. It should be considered as an ensemble of conformational states rather than as a single static structure. These new views have given impetus toward the growing interest in understanding the role of protein structural fluctuations in enzyme reactions.[8−12]

In recent years, impressive advances have been made in developing and applying combined quantum mechanical and molecular mechanical (QM/MM) methods to study enzyme reactions.[13−20] Quantum mechanical methods used range from semiempirical (AM1 or PM3) to ab initio QM methods, including Hartree−Fock, MP2 and DFT methods. To account for structural fluctuations in the protein, it would be ideal to carry out molecular dynamics or Monte Carlo simulations in which QM/MM energy and forces are evaluated at each step. In practice, this is only feasible for semiempirical QM/MM models[21,22] and EVB methods.[23,24,25] A majority of QM/MM studies of enzyme reactions are done in the following fashion: constructing the initial structure of the enzyme−substrate complex with the crystal structure and molecular modeling methods, optimizing the reactant structure and mapping out the reaction path along a predefined reaction coordinate, and then carrying out a single-point higher level B3LYP/MM or MP2/MM calculation with a larger basis set for determined reactant, transition state, and product structures to calculate the enzyme reaction barrier. Often a single starting structure is employed, with the assumption that the structure is a reasonable representation. However, the validity of such an assumption has not been examined.

The enzyme that we chose to study is acetylcholinesterase (AChE), a serine hydrolase responsible for the termination of impulse signaling at cholinergic synapses. It catalyzes the hydrolysis of the neurotransmitter acetylcholine (ACh) with a remarkably high catalytic efficiency.[26] The active site of AChE, located at the base of a long and narrow 20 Å gorge,[27] consists of two subsites: an "esteratic" subsite containing the catalytic machinery and an "anionic" subsite responsible for binding the quaternary trimethylammonium tail group of ACh.[26] For the substrate to reach the active site from the surface of the AChE, molecular dynamics simulations have revealed that the enzyme structural fluctuations play an essential role,[3,28] which open the gorge every few picoseconds to allow the passage of the substrate.

The essential catalytic functional unit of AChE is the catalytic triad consisting of Ser203, His447, and Glu334.[26] (Throughout this article, the sequence numbers follow the amino acid abbreviations of mouse AChE.) The oxyanion hole, formed by the peptidic NH groups of Gly121, Gly122, and Ala204, is another important functional unit in the esteratic subsite.[29] In the anionic subsite, site-directed mutagenesis indicates that Trp86,[30,31] Glu202,[32] and Phe337[33] play an important role in binding the quaternary trimethylammonium tail group. Our recent combined molecular dynamics simulation and multiple ligand docking studies[34] indicate that the "esteratic" and "anionic" subsites act together to achieve substrate binding specificity.

The first step of the acylation reaction, as shown in Figure 1, proceeds by nucleophilic addition of the Ser203 O attacking the carbonyl C of ACh. This reaction is facilitated by simultaneous proton transfer from Ser203 to His447, and it has been previously studied with a combined ab initio quantum mechan-

* To whom correspondence should be addressed. E-mail: yzhang@mccammon.ucsd.edu.

10.1021/jp022525e CCC: $25.00
Published on Web 04/11/2003

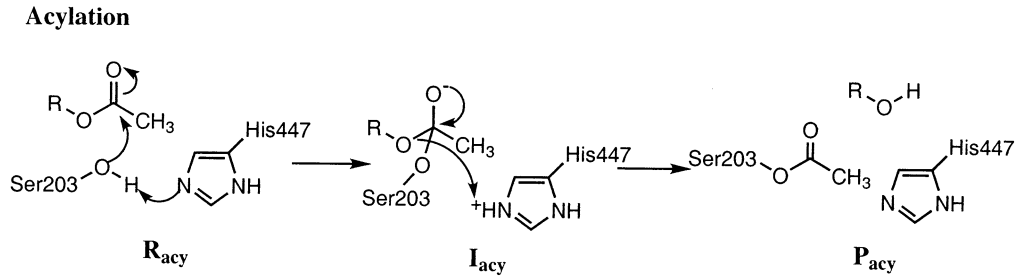

Figure 1. Acylation reaction mechanism of acetylcholine catalyzed by AChE.

TABLE 1: Energy Barriers for First Step of Acylation of ACh in AChE[a]

snapshot	HF/3-21G (small)	MP2/6-31+G* (small)	HF/3-21G (large)
020	14.0	12.6	11.6
100	14.5	12.1	11.1
200	16.4	14.0	14.5
400	17.9	16.6	15.2
500	16.1	14.6	15.4
700	13.7	12.0	12.0
800	12.1	10.6	10.2
900	12.9	11.8	10.8
average	14.7 ± 2.0	13.0 ± 1.9	12.6 ± 2.1

[a] "Small" refers to the QM/MM calculation results with a small QM subsystem, whereas "large" Refers to the QM/MM calculation results with a large QM subsystem.

ical/molecular mechanical (QM/MM) approach using a single snapshot from a 1 ns AChE−ACh MD trajectory.[35] It is found that the contribution of Glu334 to the catalytic reaction is mainly via electrostatic stabilization of the transition state. The oxyanion hole, formed by peptidic NH groups from Gly121, Gly122, and Ala204, is also found to play an important role in catalysis. In the ACh−AChE binding complex, only two hydrogen bonds are formed between the carbonyl O of ACh and the peptidic NH groups of Gly121 and Gly122. As the reaction proceeds, the distance between the carbonyl O of ACh and NH group of Ala204 becomes smaller, and the third hydrogen bond is formed in the transition state. The three hydrogen bonds are maintained as the reaction progresses to the tetrahedral intermediate. In the analysis of a 1 ns ACh−AChE MD trajectory,[34] we found that there are considerable structural fluctuations in the enzyme active site and substrate.

To account for protein dynamics and to investigate the effect of different conformations on the enzyme reaction energy barrier, we have revisited the initial step of the acylation reaction catalyzed by acetylcholinesterase (AChE) with a multiple QM/MM reaction path approach. Besides a single starting structure used in previous studies,[35] we have chosen 10 additional equally spaced snapshots from a 1ns MD trajectory as starting points for the QM/MM calculations. We found that enzyme−substrate conformation fluctuations lead to significant differences in the calculated reaction energy barrier; however, the qualitative picture of the role of the catalytic triad and oxyanion hole in AChE catalysis is very consistent.

2. Computational Methods

The multiple QM/MM minimum reaction energy path scheme consists of two main components: generating enzyme−substrate conformations with molecular dynamics simulation and mapping out the minimum energy path for each conformational snapshot with combined QM/MM calculations.

Preparation of the initial ACh−AChE complex and the details of molecular dynamics simulations and QM/MM calculations have been discussed in detail in ref 35. Here we just give a brief account. The whole ACh−AChE system consists of AChE, ACh, and 518 water molecules, a total of 9859 atoms. Because our interest focuses on the active site, only atoms within 20 Å of Ser203 O are movable during the molecular dynamics simulation and ab initio QM/MM calculations. For the QM/MM calculations, the prepared enzyme−substrate system was first partitioned into a QM subsystem and an MM subsystem. To compare the results in ref 35, two partition schemes have been used. The first utilized a smaller QM subsystem consisting of the substrate ACh and the side-chains of Ser203 and His447, with a total of 44 QM atoms. The second larger QM subsystem also included the side-chain of Glu334 leading to a total of 54 QM atoms. The boundary problem between the QM and MM subsystems was treated using the pseudobond approach.[36]

Besides the initial snapshot (referred to as 020 in the following tables and text) that we have studied with the QM/MM method, we choose 10 additional equally spaced snapshots at 100, 200, ..., 1000 ps from our 1 ns MD simulation. Each starting structure for the QM/MM studies was first minimized with the MM method. The criterion used for convergence is the root-mean-square (RMS) energy gradient being less than 0.1 kcal mol^{-1} $Å^{-1}$.

With the MM minimized ACh−AChE system, the iterative optimization procedure[37] was applied to the QM/MM system with HF/3-21G QM/MM calculations, leading to the optimized structure for the reactant. For the initial step of the acylation reaction, the reaction coordinate chosen was the simultaneous bond formation of the new C−O bond between ACh and Ser203 and the proton transfer reaction between Ser203 and His447, the same as in our previous studies. An iterative restrained minimization was then repeatedly applied to different points along the reaction coordinate, resulting in an optimum path for the reaction in the enzymatic environment and its associated potential energy surface. Stationary points obtained along the minimum energy paths and Hessian matrixes for degrees of freedom involving atoms in the QM subsystem were calculated leading to determination of the corresponding vibrational frequencies.[19] If the minimum energy path turns out to be smooth and continuous, the energy maximum on the path with one and only one imaginary frequency is the transition state, whereas the energy minimum along the path with no imaginary frequencies is characterized as the reactant or the intermediate. For the reactant, transition state, and intermediate state, we further carried out single-point high-level (MP2) QM/MM calculations with a larger 6-31+G* basis set. If the minimum energy path turns out to be not smooth or continuous, it is discarded. Among the 11 QM/MM runs, three runs (300, 600, and 1000) were discarded because of discontinuity in the reaction coordinate.

The calculations were carried out using modified versions of the Gaussian 98[38] and the TINKER programs.[39] For the QM subsystem, criteria used for geometry optimizations follow

TABLE 2: Key Ligand−Receptor Distances at Individual Reactant Conformations Calculated at the HF/3-21G QM/MM Level with the Small QM Subsystem Partition

snapshot	Ser203 O carbonyl C	Gly121 N carbonyl O	Gly122 N carbonyl O	Ala204 N carbonyl O	Trp86ring N+	Tyr337-O N+	Glu202-O N+
020	2.587	2.844	2.890	3.586	4.640	4.158	3.670
100	2.573	2.817	2.794	3.512	4.054	3.878	4.104
200	2.859	2.796	2.793	4.034	4.105	3.819	4.096
400	2.663	2.846	2.782	3.997	4.141	4.744	4.371
500	2.612	2.839	2.958	3.479	4.177	4.187	3.771
700	2.516	2.863	2.842	3.453	4.173	4.056	3.981
800	2.402	2.788	2.835	3.344	4.133	3.897	4.031
900	2.467	2.776	2.859	3.558	4.083	4.192	3.589

TABLE 3: Key Ligand−Receptor Distances at Individual Transition State Conformations Calculated at HF/3-21G QM/MM Level with the Small QM Subsystem Partition

snapshot	Ser203 O carbonyl C	Gly121 N carbonyl O	Gly122 N carbonyl O	Ala204 N carbonyl'O	Trp86ring N+	Tyr337-O N+	Glu202-O N+
020	1.704	2.870	2.973	3.159	4.563	4.229	3.717
100	1.668	2.829	2.860	3.084	4.055	3.841	4.145
200	1.669	2.781	2.832	3.354	4.115	3.828	4.140
400	1.677	2.829	2.840	3.440	4.157	4.818	4.491
500	1.711	2.882	3.100	3.063	4.182	4.190	3.780
700	1.674	2.876	2.926	3.057	4.181	4.054	3.980
800	1.702	2.813	2.909	3.053	4.149	3.918	4.062
900	1.713	2.799	2.921	3.200	4.102	4.215	3.608

TABLE 4: Electrostatics Contribution of Specific Residues to the Transition State Stabilization or Destabilization[a]

snapshot	Gly121	Gly122	Ala204	Glu334	Glu202
020	−4.0	−2.6	−4.0	−11.5	8.4
100	−4.7	−3.3	−4.1	−10.8	7.2
200	−5.7	−3.7	−3.1	−10.7	8.0
400	−4.9	−3.5	−3.0	−11.6	8.6
500	−3.6	−1.9	−4.5	−11.6	8.1
700	−4.0	−2.7	−4.4	−11.3	7.6
800	−3.7	−2.4	−3.6	−9.9	6.5
900	−3.9	−2.6	−3.3	−9.9	7.4

[a] Energy units are in kcal/mol. Negative numbers mean stabilization of the transition state, whereas positive numbers mean destabilization of the transition state.

Gaussian 98 defaults. For the MM subsystem, the criterion used is the root-mean-square (RMS) energy gradient being less than 0.1 kcal mol^{-1} Å^{-1}. In the MM minimizations, only those atoms within 20 Å of the oxygen of Ser203 are allowed to move. No cutoff for nonbonded interactions is used in the QM/MM calculations and the MM minimizations. Throughout the calculations, the pseudobonds were treated with the 3-21G basis set and its corresponding effective core potential parameters.[36] The molecular MM field used is the AMBER 95 all-atom force field[40,41] and the TIP3P model for water.[42]

3. Results and Discussion

The calculated energy barriers for the 8 runs of ACh with a smooth and continuous minimum energy path are shown in Table 1. The 020ps snapshot is the initial structure run as described in ref 35. We can see that different initial structures do lead to significant differences in the calculated reaction energy barrier. The average QM/MM reaction energy barrier is 14.7 ± 2.0 with the small QM subsystem at the level of HF-(3-21G)/MM, 13.0 ± 1.9 with the small QM subsystem at the level of MP2(6-31+G*)/MM, and 12.6 ± 2.1 for the large QM subsystem at the level of HF(3-21G)/MM. These average numbers are in good agreement with the activation barrier of ∼ 12 kcal/mol from the experimental value of k_{cat} by simple transition state theory.[26,25] Our previous results with a single starting structure (020), which are 14.0, 12.6, and 11.6 kcal/mol, are quite close to the average number. However, we can see that this is fortuitous. From the variation in energy barriers, it is obvious that any single calculation will not necessarily be close to the average. These results emphasize the importance of employing multiple starting structures rather than a single starting structure to calculate the enzyme reaction energy barrier.

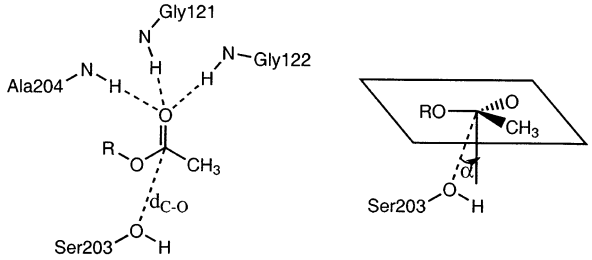

Figure 2. Esteratic binding site for the acetyl headgroup.

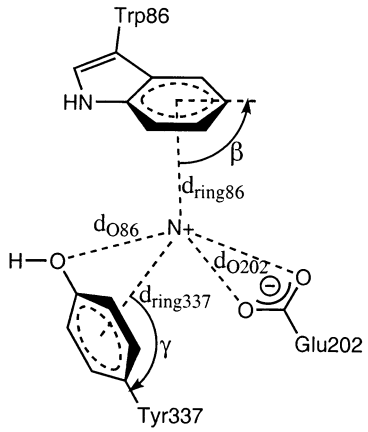

Figure 3. Anionic binding site for the tail group.

On the other hand, we can see that, although structural fluctuations strongly influence the absolute energy barrier, the barrier difference calculated with different QM methods or with different QM/MM partitions varies much less. The difference between MP2/6-31+G* QM/MM and HF/3-21G QM/MM with the small QM subsystem is −1.7 ± 0.5, and the difference between the large QM subsystem and small subsystem at HF/3-21G QM/MM level is −2.1 ± 0.8 kcal/mol. More importantly, the qualitative picture of the role of the catalytic triad and

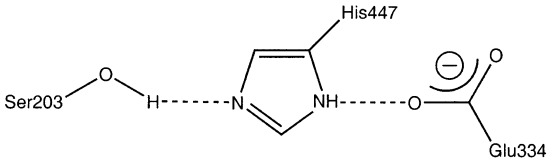

Figure 4. Hydrogen bonds in the setup of the catalytic triad.

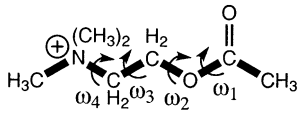

Figure 5. Schematic of dihedral angles along backbone of ACh.

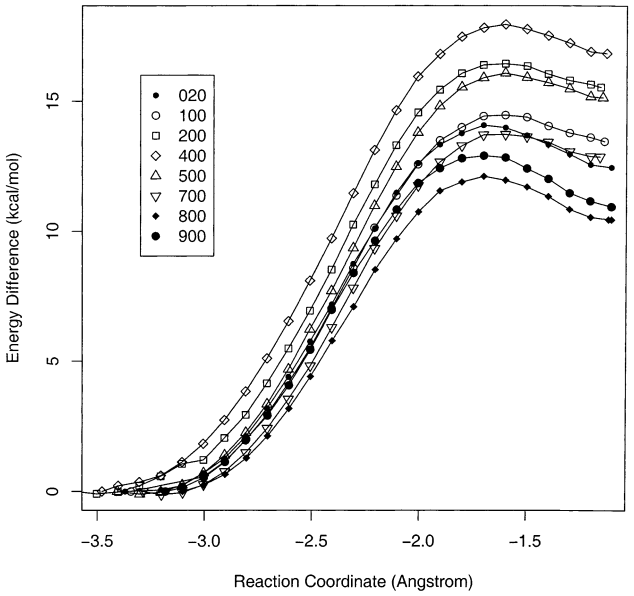

Figure 6. Individual QM/MM minimum energy paths for the first step of the acylation reaction catalyzed by AChE with different snapshots as the starting geometry. The results are for the small QM subsystem partition.

oxyanion hole in AChE catalysis remains very consistent despite different starting structures. We have already seen that treating Glu-334 quantum mechanically versus molecular mechanically only lowers the reaction barrier about 2 kcal/mol. From the geometrical data in Tables 2 and 3, all of the 8 runs show the same qualitative steps to reaction, i.e., two hydrogen bonds are formed at the initial reactant state and the third hydrogen bond is only formed at the transition state and remains in the tetrahedral intermediate. There are some small variations in how the bond distances change as the reaction proceeds, but the qualitative pictures are all consistent.

We have analyzed the energy contribution by individual residues as the reaction proceeds from reactant to transition state. The structures and charges of the transition state and the reactant were determined from HF(3-21G)/MP2(6-31+G*) QM/MM calculations with the small QM subsystem partition. The electrostatic interaction energy between the given residue and the QM subsystem was calculated classically for the transition state and reactant. The difference between the interaction energy of reactant and transition state tells us the contribution to the reaction barrier, as shown in Table 4. Negative numbers indicate that the residue lowers the reaction barrier, whereas positive numbers indicates the opposite. We can see that the picture is consistent for all 8 runs: Glu334, Gly121, Gly122, and Ala204 all play an important role in stabilizing the transition state by electrostatic interactions, whereas Glu202 destabilizes the transition state through electrostatic interactions.

TABLE 5: Some Key Geometry Elements at Individual Reactant Conformations Calculated at the HF/3-21G QM/MM Level with the Small QM Subsystem Partition[a]

snapshot	Ser203 O His447 N_ϵ	His447 N_δ Glu334 O	α	ω_1	ω_2	ω_3	ω_4
020	2.729	2.685	6.8	190.4	167.8	181.0	178.7
100	2.704	2.680	7.8	187.9	178.5	173.2	178.6
200	2.664	2.705	11.3	185.2	174.7	182.3	178.5
400	2.756	2.708	7.3	188.3	179.2	178.9	181.3
500	2.743	2.690	9.8	189.8	171.7	178.4	180.4
700	2.724	2.684	8.3	188.6	175.8	174.6	177.2
800	2.662	2.685	6.8	190.5	174.7	175.7	176.3
900	2.665	2.681	7.0	188.1	168.1	182.9	170.7

[a] Distances in angstroms. The definitions of α and ω_i, $i = 1$ and 4, are illustrated in Figures 2 and 5, respectively.

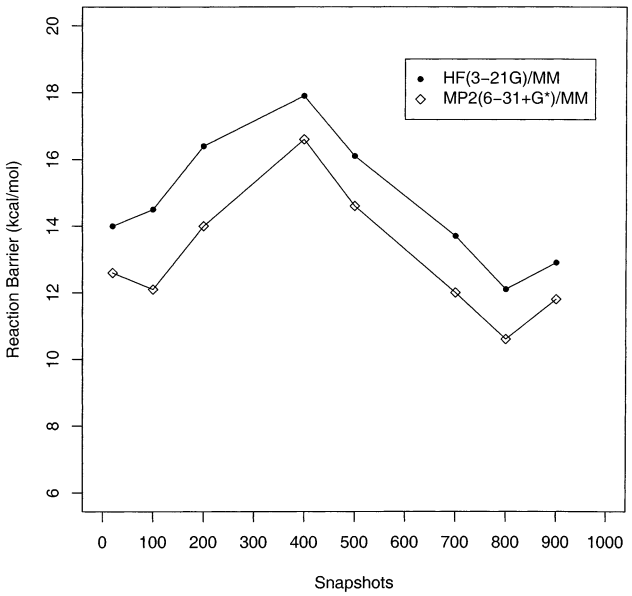

Figure 7. Individual QM/MM energy barriers for the first step of the acylation reaction catalyzed by AChE with different snapshots as the starting geometry. The results are for the small QM subsystem partition.

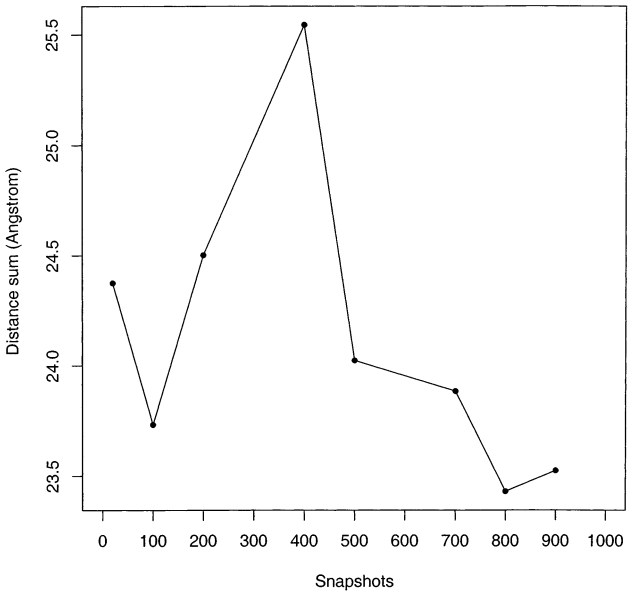

Figure 8. Sum of key ligand−receptor distances presented in Table 2.

To understand how the structural fluctuations affect the calculated reaction barrier, we have calculated some key geometry elements of the enzyme active site in QM/MM

optimized reactant structures, including ligand−receptor distances, catalytic triad setup, conformation of the substrate, and the nucleophilic attacking angle α. Illustrations of these geometry elements are presented in Figures 2−5. The calculated results are in Tables 2 and 5. Plots of the minimum energy paths and individual barriers with the small QM subsystem for ACh−AChE are shown in Figures 6 and 7, respectively. The highest barrier is at 400 ps. The lowest barriers are at 800 ps.

We can see that the value of each individual geometry element in Tables 2 and 5, whether it be a single distance or the single nucleophilic attacking angle α, does not track with the barrier height. The rises and dips in the calculated barrier (Figure 7) do show a similar qualitative trend to the tightness of binding to the substrate (Figure 8), where tightness of binding was measured as a simple distance sum of the ligand−receptor distances in Table 2. For example, the 400 ps snapshot has the largest distance sum, and the 800 ps snapshot has the shortest distance sum in Figure 8, and they have the highest and lowest calculated barriers in Figure 7, respectively. Adding extra distances representing the setup of the hydrogen bonds in the catalytic triad gives a similar qualitative picture.

4. Conclusion

To study the effect of structural fluctuations on the resulting enzyme reaction energy barrier, the initial step of the acylation reaction catalyzed by acetylcholinesterase (AChE) has been revisited with a multiple QM/MM reaction path approach. We have calculated the MP2(6-31+G*) QM/MM barrier for 8 different starting conformations obtained from a 1 ns molecular dynamics trajectory. It is found that the enzyme−substrate structural fluctuations lead to significant differences in the calculated reaction energy barrier; however, the qualitative picture on the role of the catalytic triad and oxyanion hole in AChE catalysis is very consistent. The simple average of the eight reaction barriers is 13.0 ± 1.9 kcal/mol, which is in good agreement with the activation barrier of ∼12 kcal/mol from the experimental value of k_{cat} by simple transition state theory. Our results demonstrate the importance of employing multiple starting structures in the QM/MM study of enzyme reactions and indicate that structural fluctuation is an integral part of the enzyme reaction process.

Acknowledgment. We are grateful for helpful discussions with Prof. Palmer Taylor. This work has been supported in part by grants from the NSF and NIH. Additional support has been provided by NBCR, Accelrys, and the W. M. Keck Foundation.

References and Notes

(1) Fersht, A. *Structure and mechanism in protein science: a guide to enzyme catalysis and protein folding*; W. H. Freeman and Company: New York, 1999.

(2) McCammon, J. A.; Harvey, S. C. *Dynamics of proteins and nucleic acids*; Cambridge University Press: New York, 1987.

(3) McCammon, J. A. Are molecular motions important for function? In *Simplicity and Complexity in Proteins and Nucleic Acids*; Frauenfelder, H., Deisenhofer, J., Wolynes, P. G., Eds.; Dahlem University Press: Berlin, 1999.

(4) Weiss, S. *Nat. Struct. Biol.* **2000**, *7*, 724−729.

(5) Palmer, A. G. *Annu. Rev. Biophys. Biomolec. Struct.* **2001**, *30*, 129−155.

(6) Zhuang, X. W.; Kim, H.; Pereira, M. J. B.; Babcock, H. P.; Walter, N. G.; Chu, S. *Science* **2002**, *296*, 1473−1476.

(7) Falke, J. J. *Science* **2002**, *295*, 1480−1481.

(8) Eisenmesser, E. Z.; Bosco, D. A.; Akke, M.; Kern, D. *Science* **2002**, *295*, 1520−1523.

(9) Gulotta, M.; Deng, H.; Deng, H.; Dyer, R. B.; Callender, R. H. *Biochemistry* **2002**, *41*, 3353−3363.

(10) Antoniou, D.; Caratzoulas, S.; Kalyanaraman, C.; Mincer, J. S.; Schwartz, S. D. *Eur. J. Biochem.* **2002**, *269*, 3103−3112.

(11) Hammes, G. G. *Biochemistry* **2002**, *41*, 8221−8228.

(12) Agarwal, P. K.; Billeter, S. R.; Rajagopalan, P. T. R.; Benkovic, S. J.; Hammes-Schiffer, S. *Proc. Natl. Acad. Sci. U.S.A.* **2002**, *99*, 2794−2799.

(13) Warshel, A.; Levitt, M. *J. Mol. Bio.* **1976**, *103*, 227.

(14) Singh, U. C.; Kollman, P. *J. Comput. Chem.* **1986**, *7*, 718−730.

(15) Field, M. J.; Bash, P. A.; Karplus, M. *J. Comput. Chem.* **1990**, *11*, 700−733.

(16) Bruice, T. C.; Kahn, K. *Curr. Opin. Chem. Biol.* **2000**, *4*, 540−544.

(17) Gogonea, V.; Suarez, D.; van der Vaart, A.; Merz, K. W. *Curr. Opin. Struct. Biol.* **2001**, *11*, 217−223.

(18) Field, M. J. *J. Comput. Chem.* **2002**, *23*, 48−58.

(19) Zhang, Y.; Liu, H.; Yang, W. Ab Initio QM/MM and Free Energy Calculations of Enzyme Reactions. In *Computational Methods for Macromolecules—Challenges and Applications*; Schlick, T., Gan, H. H., Eds.; Springer-Verlag: New York, 2002.

(20) Gao, J. L.; Truhlar, D. G. *Annu. Rev. Phys. Chem.* **2002**, *53*, 467−505.

(21) Liu, H.; Muller-Plathe, F.; van Gunsteren, W. F. *J. Mol. Biol.* **1996**, *261*, 454−469.

(22) Alhambra, C.; Wu, L.; Zhang, Z.-Y.; Gao, J. *J. Am. Chem. Soc.* **1998**, *120*, 3858−3866.

(23) Warshel, A. *Computer Modeling of Chemical Reactions in Enzymes*; John Wiley & Sons: New York, 1991.

(24) Aqvist, J.; Warshel, A. *Chem. Rev.* **1993**, *93*, 2523−2544.

(25) Fuxreiter, M.; Warshel, A. *J. Am. Chem. Soc.* **1998**, *120*, 183−194.

(26) Quinn, D. M. *Chem. Rev.* **1987**, *87*, 955−979.

(27) Sussman, J. L.; Harel, M.; Frolow, F.; Oefner, C.; Goldman, A.; Toker, L.; Silman, I. *Science* **1991**, *253*, 872−879.

(28) Shen, T.; Tai, K.; Henchman, R. H.; McCammon, J. A. *Acc. Chem. Res.* **2002**, *35*, 332−340.

(29) Harel, M.; Quinn, D. M.; Nair, H. K.; Silman, I.; Sussman, J. L. *J. Am. Chem. Soc.* **1996**, *118*, 2340−2346.

(30) Ordentlich, A.; Barak, D.; Kronman, C.; Flashner, Y.; Leitner, M.; Segall, Y.; Ariel, N.; Cohen, S.; Velan, B.; Shafferman, A. *J. Biol. Chem.* **1993**, *268*, 17083−17095.

(31) Quinn, D. M.; Feaster, S. R.; Nair, H. K.; Baker, N. A.; Radic, Z.; Taylor, P. *J. Am. Chem. Soc.* **2000**, *122*, 2975−2980.

(32) Radic, Z.; Gibney, G.; Kawamoto, S.; MacPhee-Quigley, K.; Bongiorno, C.; Taylor, P. *Biochemistry* **1992**, *31*, 9760−9767.

(33) Radic, Z.; Pickering, N. A.; Vellom, D. C.; Camp, S.; Taylor, P. *Biochemistry* **1993**, *32*, 12074−12084.

(34) Kua, J.; Zhang, Y.; McCammon, J. A. *J. Am. Chem. Soc.* **2002**, *124*, 8260−8267.

(35) Zhang, Y.; Kua, J.; McCammon, J. A. *J. Am. Chem. Soc.* **2002**, *104*, 10572−10577.

(36) Zhang, Y.; Lee, T.; Yang, W. *J. Chem. Phys.* **1999**, *110*, 46−54.

(37) Zhang, Y.; Liu, H.; Yang, W. *J. Chem. Phys.* **2000**, *112*, 3483−3492.

(38) Frisch, M. J.; Trucks, G. W.; Schlegel, H. B.; Scuseria, G. E.; Robb, M. A.; Cheeseman, J. R.; Zakrzewski, V. G.; Montgomery, J. A., Jr.; Stratmann, R. E.; Burant, J. C.; Dapprich, S.; Millam, J. M.; Daniels, A. D.; Kudin, K. N.; Strain, M. C.; Farkas, O.; Tomasi, J.; Barone, V.; Cossi, M.; Cammi, R.; Mennucci, B.; Pomelli, C.; Adamo, C.; Clifford, S.; Ochterski, J.; Petersson, G. A.; Ayala, P. Y.; Cui, Q.; Morokuma, K.; Malick, D. K.; Rabuck, A. D.; Raghavachari, K.; Foresman, J. B.; Cioslowski, J.; Ortiz, J. V.; Stefanov, B. B.; Liu, G.; Liashenko, A.; Piskorz, P.; Komaromi, I.; Gomperts, R.; Martin, R. L.; Fox, D. J.; Keith, T.; Al-Laham, M. A.; Peng, C. Y.; Nanayakkara, A.; Gonzalez, C.; Challacombe, M.; Gill, P. M. W.; Johnson, B. G.; Chen, W.; Wong, M. W.; Andres, J. L.; Head-Gordon, M.; Replogle, E. S.; Pople, J. A. *Gaussian 98*, revision A.5; Gaussian, Inc.: Pittsburgh, PA, 1998.

(39) Ponder, J. W. *TINKER, Software Tools for Molecular Design*, version 3.6; February 1998. The most updated version for the TINKER program can be obtained from J. W. Ponder's World Wide Web site at http://dasher.wustl.edu/tinker.

(40) Cornell, W. D.; Cieplak, P.; Bayly, C. I.; Gould, I. R.; Merz, K. M.; Ferguson, D. M.; Spellmeyer, D. C.; Fox, T.; Caldwell, J. W.; Kollman, P. A. *J. Am. Chem. Soc.* **1995**, *117*, 5179−5197.

(41) Fox, T.; Scanlan, T. S.; Kollman, P. A. *J. Am. Chem. Soc.* **1997**, *119*, 11571−11577.

(42) Jorgensen, W. L.; Chandrasekhar, J.; Madura, J.; Impey, R. W.; Klein, M. L. *J. Chem. Phys.* **1983**, *79*, 926−933.